Adaptation without parameter change: Dynamic gain control in motion detection

Alexander Borst*†, Virginia L. Flanagin*, and Haim Sompolinsky‡

*Department of Systems and Computational Neuroscience, Max Planck Institute of Neurobiology, 82152 Martinsried, Germany; and ‡Racah Institute of Physics and Center for Neural Computation, Hebrew University, Jerusalem 91904, Israel

Communicated by Donald A. Glaser, University of California, Berkeley, CA, January 20, 2005 (received for review February 19, 2002)

Many sensory systems adapt their input-output relationship to changes in the statistics of the ambient stimulus. Such adaptive behavior has been measured in a motion detection sensitive neuron of the fly visual system, H1. The rapid adaptation of the velocity response gain has been interpreted as evidence of optimal matching of the H1 response to the dynamic range of the stimulus, thereby maximizing its information transmission. Here, we show that correlation-type motion detectors, which are commonly thought to underlie fly motion vision, intrinsically possess adaptive properties. Increasing the amplitude of the velocity fluctuations leads to a decrease of the effective gain and the time constant of the velocity response without any change in the parameters of these detectors. The seemingly complex property of this adaptation turns out to be a straightforward consequence of the multidimensionality of the stimulus and the nonlinear nature of the system.

insect | model | motion vision

Adaptation is a widespread phenomenon in biological systems. Generally it may be defined as a change in the sensitivity of the system to the current stimulus after a change in the statistics of the input signal, making the system better suited to cope with the present environment. In particular, the gain of the input-output relation of sensory systems is often modified, enabling them to convey information about the relevant stimulus parameters despite changes in the statistics of the sensory environment. Such adaptation has been observed in the well studied motion detection system that underlies fly motion vision (1–3). In the motion sensitive neuron, H1, the variance of a band-limited Gaussian velocity waveform affects the neuron's velocity response relationship. This response exhibits a rather steep slope around zero velocity for small velocity fluctuations, whereas for large velocity fluctuations this slope was found to be substantially reduced (4–6). Gain control in H1 has been interpreted as adaptive rescaling set to match the dynamic range of the response to that of the stimulus and used to maximize the system's information transmission. However, the mechanism underlying this adaptation has not been elucidated.

Adaptation in sensory systems often occurs on a much slower time scale than the duration of the system's impulse response, indicating the presence of a special mechanism that slowly changes the system's response parameters integrating information about the stimulus history. H1 gain adaptation takes place on a surprisingly fast time scale: it occurs within 1 s after switching from one stimulus condition to another (5). Fast adaptation has also been observed in other neuronal sensory systems (7–9), not only in the response gain, but also in its time course (7). When the adaptation operates on the same time scale as the response itself, the separation between the mechanisms underlying the adaptation and those that give rise to the response becomes ambiguous, suggesting that the adaptation emerges naturally from the salient response properties of the system. Pursuing this hypothesis, we asked whether gain adaptation in fly motion vision could be the outcome of the intrinsic properties of the motion detection mechanism, rather than a special mechanism that changes the parameters of the system. To answer this question, we studied theoretically the adaptive properties of correlation-type motion detectors, known as Reichardt detectors, which mimic many response properties of fly motion-sensitive interneurons in surprising detail (10–14). Here, we show that changes in the response gain and the response time course can be explained by the intrinsic features of the motion detector. We argue that this automatic gain adaptation results from the inherent nonlinearity of the response of the system to a multidimensional stimulus. Thus, automatic gain control may be an integral feature of other sensory systems.

Materials and Methods

Experiments. Flies were stimulated by a moving sinusoidal wave grating (22° spatial wavelength, 63% contrast, 14 cd/m^2 mean luminance), with a low-pass filtered white noise velocity profile. The grating was presented on a cathode ray tube (Tektronix 608), 7.5 cm in front of the fly, by means of a Picasso image synthesizer (Innisfree, Cambridge, MA) at a frame rate of 200 Hz. The screen had a horizontal and vertical extent of 65° and 80°, respectively, as seen by the fly. Spikes were recorded extracellularly with a tungsten electrode inserted in the lobula plate (Fig. 1*A*), fed through a threshold device, and transferred at 1 kHz temporal resolution to a computer (Pentium II-based PC with a DAS16 I/O board from MetraByte, Tauton, MA). For each stimulus condition, ≈100 sweeps of identical stimuli, each with a duration of 9 s, were presented with a 1-s pause between them. Stimulus-response functions were constructed for a time delay equal to the maximum of the cross-correlation between the velocity waveform and the response poststimulus time histogram (4 ms binwidth). The slope of this function was determined by using a velocity range from −0.25 to 0.5 times the standard deviation of the velocity σ.

A Model of Motion Detection in H1. ***The stimulus.*** Similar to the experiment, the stimulus in the model consists of a moving sine grating of one wavelength, whose velocity $v(t)$ is expressed as a temporal frequency (in units of Hz) that reflects the number of spatial periods passing 1 image location per s. The velocity profile is generated by a low-pass filtering of white noise. We write the velocity autocorrelation as $\sigma^2 c(t)$ where $c(t) = \exp(-|t|/\tau_0)$ is the normalized autocorrelation, τ_0 is its time constant, and σ is the velocity's standard deviation. Associated with $c(t)$ we define two useful quantities:

$$C(t', t) = \int_{t'}^{t} d\tau c(\tau)$$
$$\Delta(t' - t) = \int_{t'}^{t} d\tau \int_{t'}^{t} d\tau' c(\tau - \tau'). \quad [1]$$

†To whom correspondence should be addressed. E-mail: borst@neuro.mpg.de.

www.pnas.org/cgi/doi/10.1073/pnas.0500491102

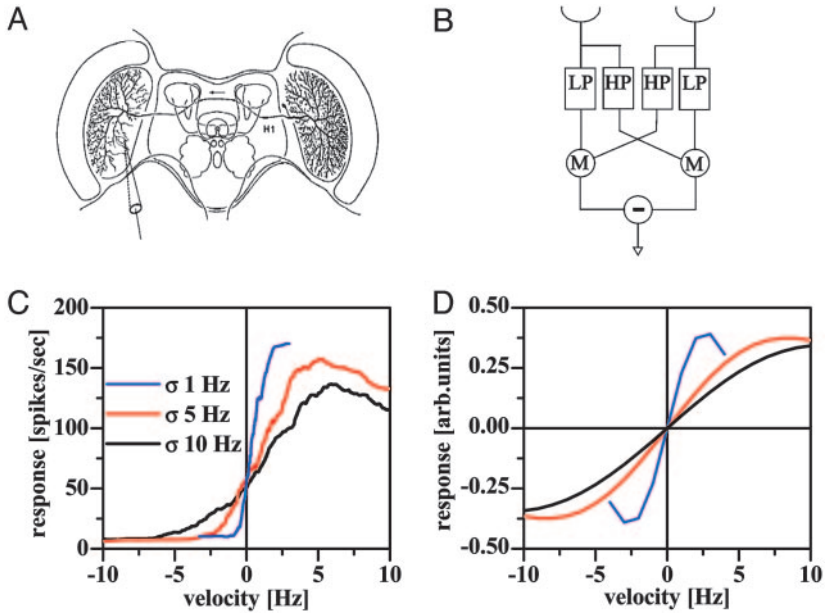

Fig. 1. Input-output relationships. (*A*) Depiction of the fly motion-sensitive interneuron H1. The fly brain is shown in a frontal section. H1 is seen to connect the lobula plates from both hemispheres. The dendrite is to the right; axonal ramifications are to the left. (*B*) A diagrammatic representation of the Reichardt detector used in the analysis. (*C*) Input-output curves from the H1 cell for three different standard deviations of the velocity fluctuations (1, 5, and 10 Hz), all with a correlation time of $\tau_0 = 0.1$ s. (*D*) Input-output curves from a simulated one-dimensional array of 25 Reichardt detectors responding to the same stimuli as used in the experiments.

Reichardt detectors. To understand how the motion vision system reacts to changes in the statistics of the stimulus velocity, we modeled H1 by an array of local motion detectors known as Reichardt detectors (1–3) (Fig. 1*B*). Reichardt detectors extract the direction of motion by multiplying the brightness signals from neighboring image locations after asymmetric temporal filtering. This operation is done twice in mirror-symmetrical subunits. As a final step, the output signals of the two subunits are subtracted. By following refs. 10–14, we used a Reichardt detector with a low-pass filter (LPF) in one input line to the multiplier with a short time constant ($\tau_L = 0.02$ s) and a high-pass filter (HPF) in the cross arm, with a time constant of $\tau_H = 0.5$ s (Fig. 1*B*). The

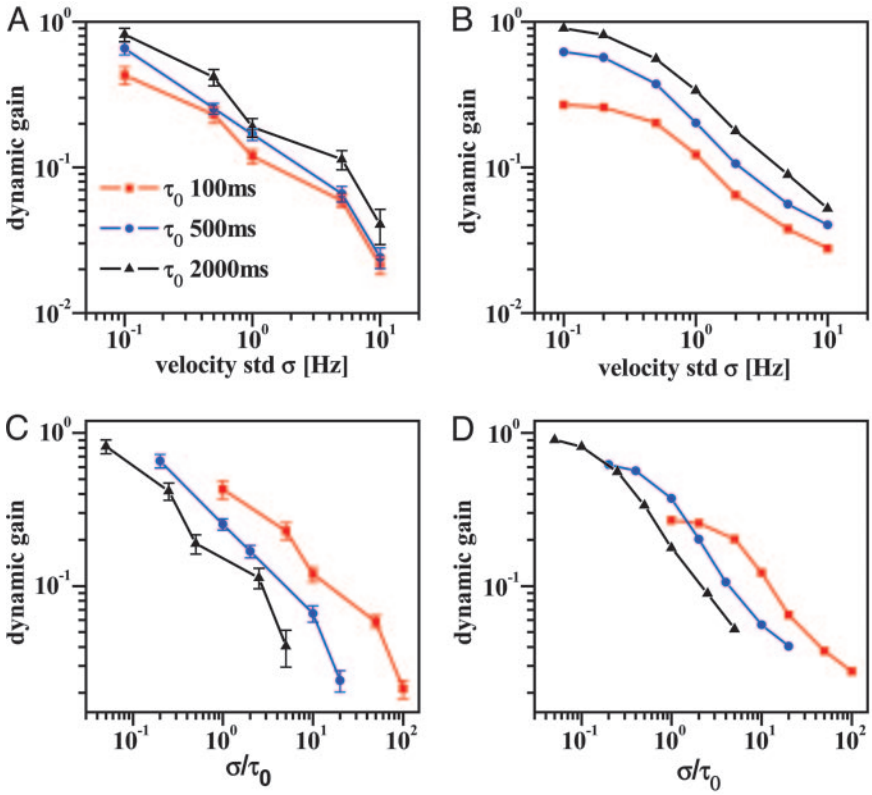

Fig. 2. Automatic gain adaptation to variance, correlation time, and acceleration. Normalized gain ($G(t)/G_{SS}$, see *Materials and Methods*) is plotted as a function of the stimulus standard deviation for three different stimulus correlation times τ_0 (0.1, 0.5, and 2.0 s). Normalized gain from experimental data (*A*) and the array of motion detectors with identical parameters (*B*) as in Fig. 1. Normalized gain of the H1 cell (*C*) and the motion detector model (*D*) as a function of the stimulus standard deviation divided by the correlation time constant, which is a measure of stimulus acceleration.

output of an array of local Reichardt detectors covering the entire visual field is given by

$$r(t) = 2\int_0^\infty d\tau \int_0^\infty d\tau' K(\tau, \tau')\sin(\Delta x(t-\tau, t-\tau')). \quad [2]$$

The time response, $K(\tau, \tau') = K_L(\tau)K_H(\tau')$ consists of the product of the LPF and HPF, which are given by $K_L(\tau) = \exp(-\tau/\tau_L)/\tau_L$ and $K_H(\tau) = d(\tau) - \exp(-\tau/\tau_H)/\tau_H$, $\tau > 0$, respectively. $\Delta x(t, t')$ is the total angular displacement of the visual pattern from time t to time t' $\Delta x(t, t') = 2\pi\int_t^{t'} d\tau v(t)$. $\Delta x(t, t')$ is Gaussian distributed with zero mean and a variance $\langle[\Delta x(t', t)]^2\rangle = (2\pi\sigma)^2\Delta(t'-t)$ (see Eq. **1**). An important quantity for this analysis is the time-lagged cross-correlation between r and v, $c_{rv}(t) = \langle r(t'+t)v(t')\rangle$, which, by using Eqs. **1** and **2**, reduces to

$$c_{rv}(t) = 4\pi\sigma^2\tau_0\int_0^\infty d\tau\int_0^\infty d\tau' K(\tau, \tau')C(t-\tau', t-\tau)$$
$$\cdot\exp[-2\pi^2\sigma^2\Delta(\tau'-\tau)]. \quad [3]$$

The Velocity Response Function. We define the response of the system $R_t(v)$ to a velocity v at time lag t as the average of the detector output r at time t, subject to the condition that the velocity at time 0 is equal to v. We call this response the "conditional response." Fixing the velocity at time 0 to v causes the mean of $\Delta x(t', t)$ to change from zero to $2\pi vC(t', t)$. Concomitantly, the variance of $\Delta x(t', t)$ is reduced to $(2\pi\sigma)^2\tilde{\Delta}(t', t)$ where $\tilde{\Delta}(t', t) = \Delta(t'-t) - (C(t, t'))^2$ (see Eq. **1**). Note that the conditional mean is proportional to the velocity at time 0, whereas the conditional variance is proportional to the variance of the velocity profile. By averaging $r(t)$ (Eq. **1**) with the conditional statistics, we obtain the conditional response:

$$R_t(v) = 2\int_0^\infty d\tau\int_0^\infty d\tau' K(\tau, \tau')\sin[2\pi vC(t-\tau, t-\tau')]$$
$$\cdot\exp[-2\pi^2\sigma^2\tilde{\Delta}(t-\tau', t-\tau)]. \quad [4]$$

From Eq. **4**, the gain of the response $G(t) = \partial R_t/\partial v|_{v=0}$ can be calculated directly. For concreteness, we will present the gain at time t, which maximizes $c_{rv}(t)$. For purposes of comparison, the gain in this study is normalized by the steady-state gain, which is the slope of the stimulus-response function at zero velocity, measured when the system has a stable output value in response to a constant stimulus. For the model in Fig. 1*b*, the steady-state gain is $G_{SS} = 4\pi\tau_H$, which can be deduced from the slope of Eq. **4** in the limit of large τ_0.

Results

Automatic Gain Adaptation in the Motion Detection System. Fig. 1*C* shows the experimentally measured velocity-response curve for different values of stimulus ensemble variance. In line with previous results, the H1 response function exhibits a significant increase in its gain when the stimulus variance is reduced. Numerical evaluation of the model velocity response function, Eq. **4**, is shown in Fig. 1*D* for several values of the stimulus variance. Importantly, the model response is strongly influenced by the variance, increasing its gain when the stimulus range of values decreases. This behavior is expected from adaptive systems, but here it occurred without any change in the system's parameters. The origin of this behavior can be understood by inspection of Eqs. **1**–**4**. The output of the motion detector at any time t is a sum of contributions from the stimuli at previous times, through $\Delta x(t-\tau, t-\tau')$ (Eq. **2**). However, the contribution of the stimulus history to the actual response is reduced by the stimulus fluctuations, as is indicated by the exponential factor in Eq. **4**. Because the amplitude of these fluctuations is proportional to σ, increasing σ suppresses the contribution to the response from previous times, resulting in a decrease in the total response.

An important prediction of our theory is that the velocity-response function should depend not only on the stimulus variance but also on its time constant, τ_0. Specifically, for a given σ, increasing τ_0 increases $C(t', t)$ and decreases $\tilde{\Delta}(t', t)$, leading to an increase of the response and its gain (see Eq. **4**). When τ_0 is large compared with the motion detector time constants τ_L and τ_H, the stimulus is essentially constant during the response period; hence, the gain approaches the steady-state value. These results are summarized in Fig. 2*A*, which presents the value of the velocity response gain as a function of the fluctuation amplitude, σ, for several values of τ_0. As shown in Fig. 2*B*, the model predictions agree nicely with the experimental results for the gain of the H1 velocity response for the same values of stimulus parameters. Although increasing σ and τ_0 have opposite effects on the gain, the reduction of the gain by increasing σ is only partially offset by a concomitant increase in τ_0. Thus, as can be concluded from Fig. 2 *C* and *D*, the gain depends not only on the acceleration σ/τ_0 but also on the higher-order time derivatives of the velocity profile.

Adaptation of the Motion Detection Time Scale. We also examined whether our motion detection model exhibits automatic changes in the time course of its output, in response to changes in the variance of the stimulus. We addressed this question by calcu-

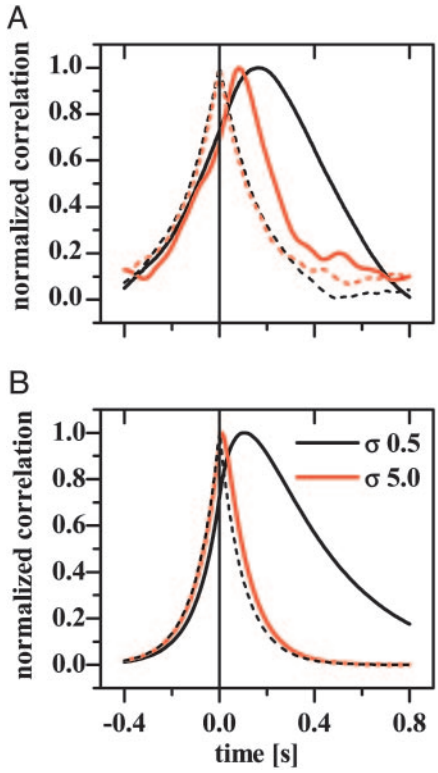

Fig. 3. Adaptation of the motion detection time scale. Stimulus-response cross-correlations from experimental data (*A*) and from the model (*B*) (see Eq. **3**). In both cases, the correlation time of the stimulus is held constant at 0.1 s, and the standard deviation of the stimulus shown here are 0.5 (black) and 5.0 Hz (red). Dotted lines represent the normalized stimulus autocorrelation function for each standard deviation.

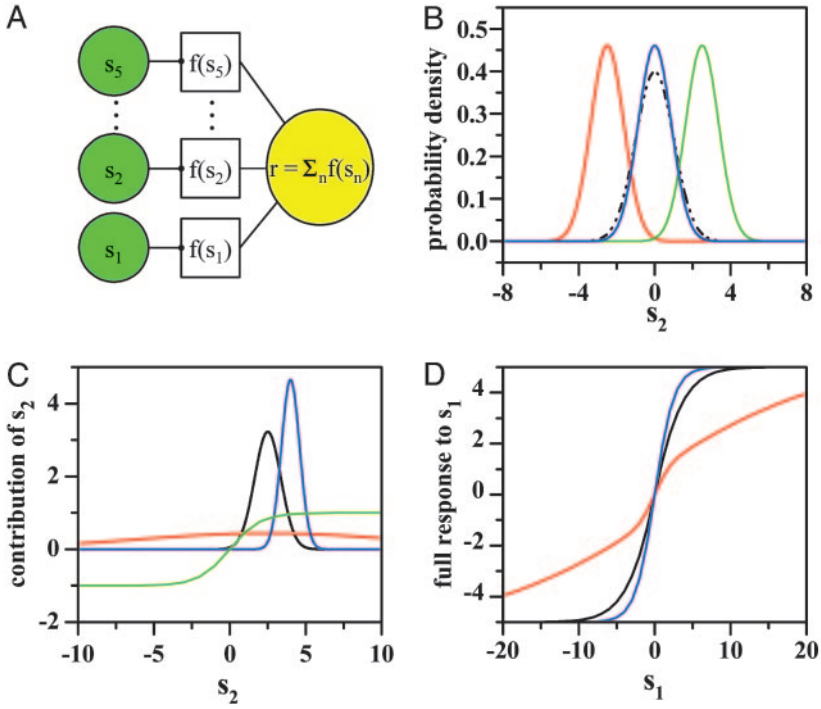

Fig. 4. Mechanism for automatic gain control. (*A*) Schematic representation of a model neuron responding nonlinearly to a multidimensional stimulus. In this example, we chose five Gaussian distributed stimulus components, with identical variance σ^2 and correlation coefficients, c. $f(s) = \tanh(s)$. (*B*) Effect of one stimulus component, s_1, on the probability distribution of a second component, s_2. Fixing the value of s_1 changes the distribution of s_2 because the two variables are correlated. The conditional distribution is narrower than the original by a factor $\sqrt{1 - c^2}$, where c is the correlation coefficient of s_1 and s_2 and is centered on cs_1. Here, $c = 0.5$. The dashed curve is the original Gaussian probability density of s_2 with $\sigma = 1$. The solid curves are the conditional densities with $s_1 = 0$ (blue), -5.0 (red), and 5.0 (green). (*C*) Contribution of s_2 to the response of s_1. The indirect response is computed by averaging $f(s_2)$ (green curve) with the conditional distribution of s_2 with ($c = 0.5$, $\sigma = 10$, red), ($c = 0.5$, $\sigma = 1$, black), and ($c = 0.8$, $\sigma = 1$, blue). In all cases, $s_1 = 0.5$. (*D*) Full response of the neuron to s_1, consisting of the direct contribution $f(s_1)$ and the indirect contributions from the other four units (similar to that described in *C*). Parameters are $c = 0.5$, $\sigma = 1$, black; $c = 0.5$, $\sigma = 10$, red; and $c = 0.8$, $\sigma = 1$, blue.

lating the time-delayed cross-correlation of the motion detection output and the stimulus, $c_{rv}(t)$ (Eq. **3**) for different values of σ. Remarkably, the time dependence of the stimulus-response correlation is sensitive to the value of σ, as shown in Fig. 3 *A* and *B*. For small σ, $c_{rv}(t)$ is peaked at the positive value of delay and has a large width around it. On the other hand, for large σ, $c_{rv}(t)$ has a narrow, nearly symmetrical profile at about zero delay. The experiments show a larger shift in the peak of the cross-correlation than the model. This finding may be due to an additional fixed delay between the retinal input and the output of the H1 cell that is absent in the model. As in the case of the gain, the automatic shortening of the time scales of the motion detection response originates from the fact that, as the velocity variance increases, the contributions to the response from previous times are suppressed. Hence, whereas for small σ, the time constants of the motion detector temporal filters contribute substantially to the time course of the output, at large σ, the time scale in the response is just the time constant of the correlations in the stimulus itself, as shown in Fig. 3.

Mechanism of Automatic Gain Control by Stimulus Variance. Contrary to the commonly accepted view that gain control requires manipulation of the response parameters, gain control occurs in a Reichardt motion detector without changing any of the system's parameters. This finding raises the interesting question of whether automatic gain adaptation to stimulus variance is specific to motion detection or whether it could be a more general feature at work in other sensory systems. In fact, we argue that our results are a natural consequence of the inherent high dimensionality of the stimulus and the intrinsic nonlinearity of the response. To demonstrate this point, we present a simple abstract model neuron responding nonlinearly to a multidimensional stimulus (Fig. 4*A*). The stimulus ensemble consists of several correlated multivariate Gaussian variables, s_i. The correlations between the different s_i may originate from the statistics of the sensory sources or from a mixing of uncorrelated stimuli by preceding neural filtering. The s_i pass through nonlinear squashing transfer functions, $f(s_i)$, and are summed linearly at the output stage. A simple one-dimensional account of the response of the neuron is generated by evaluating the average output of the neuron conditioned on fixing one of the stimulus variables, say s_1. Changing the value of s_1 modifies the residual probability distribution of the other stimulus variables (Fig. 4*B*). Thus, the neuron's response to s_1 consists not only of the direct response $f(s_1)$ but also of contributions coming from the other stimulus variables $f(s_i)$ (Fig. 4*C*). This contribution varies with both the amplitude of the stimulus fluctuations as well as with the amount of correlations between s_1 and s_i. Increasing the amplitude and decreasing the correlations decrease the gain of the indirect response (Fig. 4*D*), and thereby also that of the total response. The degree of this gain control depends on the number of stimulus variables, s_i, and the strength of their correlations with s_1. In the case of the motion detection, the different s_i corresponds to the velocities (or displacements) at different times, with correlations that depend on their time difference relative to τ_0. The nonlinearity corresponds to the dependence of the response on the global velocity signal (e.g., sinusoidal in the present experiment, see Eq. **1**). This result explains both the decrease of the gain of the motion detector with increasing σ and the increase of the dynamic gain with increasing correlation time of the stimulus, τ_0. The generic nature of the architecture of Fig. 4 suggests that a similar mechanism may underlie other phenomena of fast adaptation in sensory systems, such as the fast component of contrast adaptation in the vertebrate retina (12).

Discussion

Gain control in H1 and other sensory systems has often been considered from a "black-box" type approach as reflecting the matching of the dynamic range of the response of the sensory system to the dynamic range of the stimulus, thereby optimizing the information transmission of the system (4, 5). Our work shows that by considering the internal structure of the black box, one obtains a richer understanding of its adaptive behavior. First, we have shown that correlation-based motion detection systems exhibit gain control of their velocity-response curve that does not require any change in the system parameters. By analytical evaluation of a model motion detection system, we show that increasing the amplitude of the velocity fluctuations

suppresses the contribution of the stimulus past, which leads to a marked reduction in the response gain. Analyzing a more general network model of sensory processing, we demonstrate that this automatic gain control is due to the intrinsic nonlinearity of the system and the high dimensionality of the stimulus ensemble. Our theory furthermore predicts that the stimulus statistics also affect the effective time scale of the system. Increasing the stimulus variance shortens the time scale of the motion detection response and reduces it to the correlation time of the stimulus fluctuations. The predicted modulation of the gain and the time course of the velocity response by the stimulus statistics is in qualitative agreement with the behavior of the fly visual interneuron H1.

Our theory reveals the natural limitations of the system's gain control. As is evident from Fig. 2*B*, although the gain increases as the stimulus standard deviation, σ, decreases, it is predicted to saturate smoothly to a finite value at low σ. The predicted gain saturation is in accordance with the experimental results (Fig. 2*A*). In contrast, the naïve information theoretic approach predicts that the adaptive gain should increase as the inverse of σ, for low σ. Finally, our theory relates the changes in the gain and time constant to the intrinsic nonlinearity of the system. Therefore, changing the form of the nonlinearity may have significant effects on the magnitude of the resultant adaptive response. Interestingly, in the H1 system, the nonlinearity can be modified by changing the wave form of the moving grating itself. Thus, we predict that the fast adaptation in H1 should be sensitive to changes in the spatial pattern of the light stimulus.

H1 exhibits a variety of adaptation phenomena in addition to those described in this work. For instance, the time constant of its impulse response shortens when the transient stimulus is applied after a previous step velocity. The sensitivity of this adaptation to the contrast of the adaptive stimulus and its local nature may indicate that the present model of motion detection does not account for this phenomenon. It should be noted that our model of H1 processing is an analog model, which does not include spiking outputs. Thus, it can be considered as a model of the input to H1 (15, 16). The subsequent transformation of this signal to spiking discharge represents an additional layer of nonlinearity that may also contribute to the fast adaptation studied in this work and other adaptation phenomena in H1. Indeed, recent modeling work has shown that spike generation nonlinearity can give rise to certain forms of fast adaptation (17, 18).

The nervous system reveals a variety of adaptive behaviors that undoubtedly involve multiple mechanisms operating on different time scales. This work shows that adaptive behaviors that operate on the same time scales as the response itself may be the natural outcome of the inherent nonlinearities of the system.

We thank Yong Choe, Juergen Haag, and Dierk Reiff for their careful reading of the manuscript, and Henry Abarbanel, Stephen Baccus, Naama Brenner, Markus Meister, and Sebastian Seung for insightful discussions. H.S. is partially supported by a U.S.–Israel Binational Science Foundation grant and funding from the Volkswagen Foundation.

1. Reichardt, W. (1961) in *Sensory Communication*, ed. Rosenblith, W. A. (MIT Press and Wiley, New York), pp. 303–317.
2. Poggio, T. & Reichardt, W. (1973) *Kybernetik* **13,** 223–227.
3. Reichardt, W. (1987) *J. Comp. Physiol. A* **161,** 533–547.
4. Brenner, N., Bialek, W. & de Ruyter van Steveninck, R. (2000) *Neuron* **26,** 695–702.
5. Fairhall, A. L., Lewen, G. D., Bialek, W. & de Ruyter van Steveninck, R. (2001) *Nature* **412,** 787–792.
6. Borst, A. (2003) *J. Comput. Neurosci.* **14,** 23–31.
7. Baccus, S. A. & Meister, M. (2002) *Neuron* **36,** 909–919.
8. Kennedy, H. J., Evans, M. G., Crawford, A. C. & Fettiplace, R. (2003) *Nat. Neurosci.* **6,** 832–836.
9. Müller, J. R., Metha, A. B., Krauskopf, J. & Lennie, P. (1999) *Science* **285,** 1405–1408.
10. Egelhaaf, M. & Reichardt, W. (1987) *Biol. Cybern.* **56,** 69–87.
11. Egelhaaf, M. & Borst, A. (1989) *J. Opt. Soc. Am. A* **6,** 116–127, and erratum (1990) **7,** 172.
12. Single, S. & Borst, A. (1998) *Science* **281,** 1848–1850.
13. Reisenman, C., Haag, J. & Borst, A. (2003) *Vis. Res.* **43,** 1293–1309.
14. Borst, A., Reisenman, C. & Haag, J. (2003) *Vis. Res.* **43,** 1311–1324.
15. Borst, A., Egelhaaf, M. & Haag, J. (1995) *J. Comput. Neurosci.* **2,** 5–18.
16. Single, S., Haag, J. & Borst, A. (1997) *J. Neurosci.* **17,** 6023–6030.
17. Chance, F. S., Abbott, L. F. & Reyes, A. D. (2002) *Neuron* **35,** 773–782.
18. Yu, Y. & Lee, T. S. (2003) *Phys. Rev. E. Stat. Nonlin. Soft Matter Phys.* **68,** 011901.